

Preoperative surgical risk assessment by evaluation of tumor blood flow using perfusion imaging by computed tomography in transsphenoidal surgery for pituitary adenoma

Nakamasa Hayashi (✉ n.hayashi@scchr.jp)

Shizuoka Cancer Center Hospital <https://orcid.org/0000-0003-4170-7304>

Koichi Mitsuya

Shizuoka Cancer Center Hospital

Shoichi Deguchi

Shizuoka Cancer Center Hospital

Atsushi Urikura

Shizuoka Cancer Center Hospital

Masahiro Endo

Shizuoka Cancer Center Hospital

Research article

Keywords: CT, Perfusion study, Pituitary adenoma, Postoperative complication, Suprasellar extension, Transsphenoidal surgery

Posted Date: July 16th, 2020

DOI: <https://doi.org/10.21203/rs.3.rs-39578/v2>

License:  This work is licensed under a Creative Commons Attribution 4.0 International License.

[Read Full License](#)

Abstract

Background: Complete removal of large and giant pituitary adenomas (PAs) with suprasellar extension by transsphenoidal surgery (TSS) is sometimes difficult. Swelling and bleeding of a residual suprasellar tumor after incomplete removal via TSS can compress the surrounding neurovascular structures, resulting in postoperative complications. We measured PA blood flow by perfusion computed tomography (PCT) and assessed its usefulness in the preoperative prediction of postoperative hemorrhagic complications after TSS.

Method: We performed PCT in 28 patients with PAs with suprasellar extension before TSS. Perfusion studies were performed with a 320-row multidetector computed tomography system. We measured cerebral blood volume (CBV) and cerebral blood flow (CBF) of the tumor (CBVt and CBFt) and normal-appearing white matter (CBVw and CBFw).

Results: In all patients, CBVt was greater than CBVw. There was a statistically significant difference between CBFt and CBFw ($p < 0.0001$). The patients were divided into 2 groups according to CBFt: high CBF (CBFt > mean value) and low CBF (CBFt < mean value). There were no statistically significant differences between the 2 groups in terms of gender, age, maximum tumor diameter, suprasellar extension grade, and extent of resection. Two of the 7 patients in the high CBF group suffered from visual acuity deterioration and visual field stenosis due to postoperative hemorrhage, while no patients in the low CBF group did ($p = 0.014$).

Conclusions: PCT may be useful in the preoperative prediction of postoperative residual tumor hemorrhage, which can be a hazardous postoperative complication after TSS for large and giant PAs.

Introduction

Transsphenoidal surgery (TSS) is often the first choice for the treatment of most pituitary adenomas (PAs) [4, 10, 11, 16]. However, the removal of large and giant PAs with suprasellar extension is sometimes difficult [6, 13, 17]. Insufficient transsphenoidal resection puts patients at risk of postoperative bleeding, edema, and increased mass effect of the residual tumor.

Perfusion imaging by computed tomography (PCT) reflects blood flow and capillary condition, making it valuable in the assessment of brain tumors. PCT has been reported to be useful in grading gliomas [2, 19], differentiating tumor prognosis from treatment-induced effects [7], and differentiating glioblastomas, lymphomas, and metastatic tumors [15]. We measured the cerebral blood volume (CBV) and cerebral blood flow (CBF) of PAs to assess tumor vascularization and evaluated the association of elevated CBV and CBF with the incidence of postoperative hemorrhage after TSS for PAs.

Methods

Patients

This retrospective study was approved by the institutional review board of the Shizuoka Cancer Center, and the requirement for informed consent was waived. All methods were performed in accordance with relevant guidelines and regulations.

We included 28 patients with PAs treated by TSS at the Shizuoka Cancer Center from March 2015 to December 2019. There were 12 men and 16 women between 29 and 84 years of age (mean age: 56.8 years).

Image Acquisition

PCT was performed before surgery using a 320-row multidetector computed tomography system (Aquillion ONE; Canon Medical Systems, Tochigi, Japan). Seven seconds after intravenously injecting 50 mL (5 mL/s) of a nonionic contrast medium (Iomeron, 350 mg/mL; Bracco-Eisai, Tokyo, Japan) using a power injector, dynamic scanning was started, and tissue attenuation of the contrast medium was monitored.

Acquired data were analyzed using the delay-insensitive singular value decomposition plus perfusion algorithm on the computed tomography scanner console. The CBV, CBF, mean transit time, and time to peak were displayed automatically. Regions of interest were placed manually at the tumor and normal-appearing white matter.

A total of 23 dynamic scans were performed for each patient, and radiation doses for PCT were 157.5 mGy per the volume computed tomography dose index and 2520 mGy·cm per the dose length product.

Statistical Analysis

Analyses were performed using version 11 of the JMP[®] software (SAS Institute Inc., Tokyo, Japan). The differences in CBV and CBF between the tumor (CBV_t and CBF_t) and normal-appearing white matter (CBV_w and CBF_w) were compared by the Wilcoxon rank sum test. Clinical characteristics were compared using the chi-square test. $P < 0.05$ was considered statistically significant.

Results

CBV_t ranged from 3.0 to 8.7 (5.1 ± 1.3) mL/100 g, and CBV_w ranged from 1.5 to 2.7 (2.0 ± 0.3) mL/100 g. In all patients, CBV_t was greater than CBV_w. There was a statistically significant difference between CBV_t and CBV_w ($p < 0.0001$; Fig. 1A).

CBF_t ranged from 28.4 to 133.2 (51.3 ± 27.7) mL/min/100 g, and CBF_w ranged from 18.4 to 31.3 (24.1 ± 3.6) mL/min/100 g. There was a statistically significant difference between CBF_t and CBF_w ($p < 0.0001$; Fig. 1B). The patients were divided into 2 groups according to CBF_t: high CBF (CBF_t > mean value; Fig. 2A) and low CBF (CBF_t < mean value; Fig. 2B).

Clinical characteristics, maximum tumor diameters, suprasellar extension grades [12, 17], and incidence of postoperative hemorrhage are summarized in Table 1. In the high CBF group, there were 2 men and 5 women between 46 and 67 years of age (mean age: 50 years). In the low CBF group, there were 10 men and 11 women between 29 and 84 years of age (mean age: 59 years). Total tumor removal was achieved in 9 patients (43%) in the low CBF group and 1 patient (14%) in the high CBF group. There were no statistically significant differences between the 2 groups regarding the maximum tumor diameter, suprasellar extension grade, and extent of resection. Two of the 7 patients in the high CBF group suffered from visual acuity deterioration and visual field stenosis due to postoperative hemorrhage, while no patients in the low CBF group did ($p = 0.014$).

Table 1. Clinical characteristics of 28 patients grouped according to tumor blood flow				
		High CBF	Low CBF	p
Number		7	21	
Mean age		50	59	0.23
Gender	Male	2	10	0.37
	Female	5	11	
Functioning adenoma		2	3	0.41
Mean maximum diameter (mm)		30	30	0.95
Grade according to suprasellar extension	A	1	5	0.57
	B	3	9	
	C	3	5	
	D	0	2	
Extent of resection	Total	1	9	0.09
	Subtotal	0	3	
	Partial	6	9	
Postoperative hemorrhage		2	0	0.014

A representative case with high CBFt is shown in Figure 3. A preoperative gadolinium-enhanced coronal T1-weighted image (Fig. 3A) shows a PA with suprasellar extension (Grade C). The scaled color maps for CBV (Fig. 3C) and CBF (Fig. 3D) show greater CBV and CBF of the tumor (6.6 and 77.5, respectively) than of the normal-appearing white matter (1.9 and 18.4, respectively). A postoperative gadolinium-enhanced coronal T1-weighted image (Fig. 3B) shows expansion of the tumor due to postoperative hemorrhage.

Discussion

There are 4 grades of PA with suprasellar extension: 1) Grade A, 0- to 10-mm suprasellar extension occupying the suprasellar cistern; 2) Grade B, 10- to 20-mm suprasellar extension with elevation of the third ventricle; 3) Grade C, 20- to 30-mm suprasellar extension occupying the anterior third ventricle; and 4) Grade D, > 30-mm suprasellar extension beyond the foramen of Monro or a Grade C tumor with lateral

extension [12]. There is a 39.5% risk of residual or recurrent tumors after an initial TSS on imaging for Grade C and D adenomas [12]. Based on their prospective study, Honegger et al. reported that vertical intracranial extension was the strongest independent predictor of incomplete resection after TSS for PAs with suprasellar extension [6]. A residual suprasellar tumor can cause postoperative hemorrhage, which can result in compression of the optic pathway and acute hydrocephalus [13, 20, 21]. Mortini et al. reported that complete giant PA removal was obtained in only 13 of 67 patients (19%) after an initial TSS [13]. Swelling and bleeding of a residual suprasellar tumor or sellar hematoma occurred in 8 of 85 patients (9%) treated by TSS. Saito et al. recommended that the intrasellar dead space and sellar floor not be reconstructed in patients undergoing subtotal or partial tumor removal during an initial TSS in an intentionally staged operation, allowing marked descent of the diaphragma sellae and suprasellar tumor, thus avoiding postoperative complications [17]. Zoda et al. reported that an open craniotomy might be selected as the initial operation in cases with the following factors: significant suprasellar extension, lateral extension, retrosellar extension, brain invasion with edema, firm tumor consistency, involvement or vasospasm of the arteries of the circle of Willis, and optic apparatus encasement or optic foramina invasion [21].

A combined simultaneous transsphenoidal and transcranial approach to large-to-giant PAs has been adopted to maximize tumor excision and lower the risk of swelling and bleeding of the residual tumor [1, 3, 9]. Han et al. reported that a simultaneous open craniotomy approach should be prepared for surgical management of giant PAs, if a tumor had 1 or more of the following characteristics: dumbbell shape; irregular shape with significant subfrontal, temporal, or intraventricular extension; previous surgical treatment; suspicious fibrous consistency; or encasement of the optic apparatus and/or cerebral arteries [5]. Nagata et al. introduced a fully endoscopic combined endonasal-supraorbital keyhole approach for complicated parasellar lesions. They demonstrated that the intraoperative endoscopic view from the supraorbital approach showed the suprasellar pituitary tumor became hyperemic and swollen, with progression of tumor debulking from the transsphenoidal approach [14]. Because neurosurgeons cannot be aware of this phenomenon when using the transsphenoidal route alone, the swelling tumor compresses the surrounding neurovascular structures, resulting in postoperative complications.

In the present study, we demonstrated that PAs had high CBVt and increased vascular density. Our results revealed that we could preoperatively identify patients with a high risk of postoperative hemorrhage from residual tumors based on high CBFt by PCT. Conversely, PAs with low CBFt, even those with Grade C or D suprasellar extension, could be safely removed via TSS as an initial surgery.

Sakai et al. reported that arterial spin-labeled perfusion images from a 3T magnetic resonance scanner reflected the vascular density of nonfunctioning PAs, which may be useful in the preoperative prediction of intra- and postoperative tumor hemorrhage [18]. PCT provides reliable information on tumor vasculature [2]. The linear relationship between attenuation changes on computed tomography and tissue concentration of contrast medium, as well as the lack of confounding sensitivity to flow artifacts, allow PCT to potentially offer a more accurate representation of tissue microvasculature than similar magnetic resonance perfusion studies [8]. Additionally, the use of PCT using a 320-row multidetector

computed tomography system in the present study overcame the limitation of limited area of coverage by conventional PCT compared with magnetic resonance perfusion imaging.

The present study has limitations that are inherent to its retrospective design. In addition, our study included a relatively small number of cases of large and giant PAs.

Conclusions

PCT may be useful in the preoperative prediction of postoperative residual tumor hemorrhage, which can lead to hazardous postoperative complications after TSS for large and giant PAs. In cases of PAs with large suprasellar extension and high CBFT, an open craniotomy might be considered in combination with TSS.

List Of Abbreviations

CBF: cerebral blood flow; CBV: cerebral blood volume; PA: pituitary adenoma; PCT: perfusion computed tomography; TSS: transsphenoidal surgery

Declarations

Ethics approval and consent to participate

Approval for this study was obtained from the institutional research ethics board of Shizuoka Cancer Center (30-J93-30-1-3). Individual written informed consent was waived because this study was retrospective in design and based on clinical records.

Consent for publication

Not applicable.

Availability of data and material

The datasets analysed during the current study are available from the corresponding author on reasonable request.

Competing interest

The authors declare that they have no competing interests.

Funding

This work has not been funded.

Author Contributions

NH designed the study, and collected data with AU. NH, KM, and SD participated in statistical analysis. NH and ME interpreted results, and prepared and drafted the manuscript. All authors read and approved the final manuscript.

Acknowledgements

Not applicable.

References

1. Alleyne CH, Barrow DL, Oyesiku NM (2002) Combined transsphenoidal and pterional craniotomy approach to giant pituitary tumors. *Sur Neurol* 57: 380-90
2. Beppu T, Sasaki M, Kudo K, Kurose A, Takeda M, Kashimura H, kashamura H, Ogawa A, Ogasawara K (2011) Prediction of malignancy grading using Computed tomography perfusion imaging in nonenhancing supratentorial gliomas. *J Neurooncol* 103: 619-27
3. D'Ambrosio AL, Syed ON, Grobelny BT, Freda PU, Wardlaw S, Bruce JN (200) *Pituitary* 12:217-215
4. Dehdashti AR, Ganna A, Karabatsou K, Gentili F (2008) Pure endoscopic endonasal approach for pituitary adenoma: early surgical results in 200 patients and comparison with previous microsurgical series. *Neurosurgery* 62: 1006-1015
5. Han S, Gao W, Jing Z, Wang Y, Wu A (2017) How to deal with giant pituitary adenomas: transphenoidal or transcranial, simultaneous or two-staged? *J Neurooncol* 132: 313-321
6. Honegger J, Ernemann U, Psaras T, Will B (2007) Objective criteria for successful transsphenoidal removal of suprasellar nonfunctioning pituitary adenoma. A prospective study. *Acta Neurochir (Wien)* 149: 21-29
7. Jain R, Scarpace L, Ellika S, Schltz LR, Rock JP, Rosenblum ML, Patel SC, Lee TY, Mikkelsen T (2007) First-pass perfusion computed tomography: Initial experience in differentiating recurrent brain tumors from radiation effects and radiation necrosis. *Neurosurgery* 61: 778-787
8. Jain R, Ellika SK, Scarpace L, Schltz LR, Rock JP, Gutierrez J, Patel SC, Ewing J, Mikkelsen T (2008) Quantitative estimation of permeability surface-area product in astroglial brain tumors using perfusion CT and correlation with histopathologic grade. *Am J Neuroradiol* 29: 694-700
9. Leung GTK, Law HY, Hung KNH, Fan YW, Lui WM (2011) Combined simultaneous transcranial and transsphenoidal resection of large-to-giant pituitary adenomas. *Acta Neurochir (Wien)* 153:1401-1408
10. Magro E, Graillon T, Lassave J, Casinetti F, Boissonneau S, Tabouret E, Fuentes S, Velly L, Gras R, Dufour H (2016) Complications related to the endoscopic endonasal transsphenoidal approach for nonfunctioning pituitary macroadenomas in 300 consecutive patients. *World Neurosurg* 89: 442-453
11. Mamelak AN, Carmichael J, Bonert VH, Cooper O, Melmed S (2013) Single-surgeon fully endoscopic endonasal transphenoidal surgery: outcomes in three-hundred consecutive cases. *Pituitary* 16: 393-401

12. Mohr G, Hardy J, Comtois R, Beauregard H (1990) Surgical management of giant pituitary adenomas. *Can J Neurol Sci* 17: 62-66
13. Mortini P, Barzaghi R, Losa M, Boari N, Giovanelli M (2007) Surgical treatment of giant pituitary adenomas: strategies and results in a series of 95 consecutive patients. *Neurosurgery* 60: 993-1004
14. Nagata Y, Watanabe T, nagatani T, Takeuchi K, Chu J, Wakabayashi T (2018) Fully endoscopic combined transsphenoidal and supraorbital keyhole approach for parasellar lesion. *J Neurosurg* 128: 685-694
15. Onishi S, Kajiwara Y, Takayasu T, Kolakshyapati M, Ishifuro M, amitya VJ, Takeshima Y, Sugiyama K, Kurisu K, Yamasaki F (2018) Perfusion computed tomography parameters are useful for differentiating glioblastoma, lymphoma and metastasis. *World Neurosurg* 119: e890-e897
16. Powell M (2012) Microscope transphenoidal surgery. *Acta Neurochir (Wien)* 154: 913-917
17. Saito K, Kuwayama A, Yamamoto N, Sugita K (1995) The transsphenoidal removal of nonfunctioning pituitary adenomas with suprasellar extension: The open sella method and intentionally staged operation. *Neurosurgery* 36: 668-676
18. Sakai N, Koizumi S, Yamashita S, Takehara Y, Sakahara H, Baba S, Oki Y, Hiramatsu H, namba H (2013) Arterial spin-labeled perfusion imaging reflects vascular density in nonfunctioning pituitary macroadenoma. *Am J Neuroradiol* 34: 2139-43
19. Shankar JJ, Woulfe J, Silva VD, Nguyen TB (2013) Evaluation of perfusion CT in grading and prognostication of high-grade gliomas at diagnosis: a pilot study. *AJR Am J Roentgenol* 200: W504-9
20. Sinha S, Sharma BS (2010) Giant pituitary adenomas – An enigma revisited. Microsurgical treatment strategies and outcome in a series of 20 patients. *British Journal of Neurosurgery* 24: 31-39
21. Zada G, Du R, Laws Jr ER (2011) Defining the “edge of the envelope”: patient selection in treating complex sellar-based neoplasms via transsphenoidal versus open craniotomy. *J Neurosurg* 114: 286-300

Figures

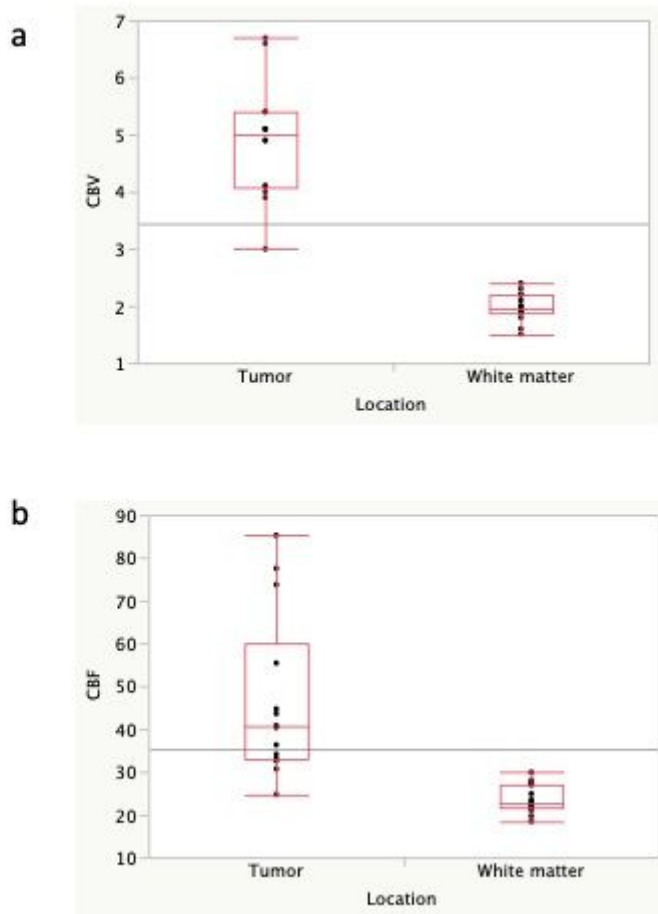


Figure 1

Box-and-whisker plots of CBV (a) and CBF (b) The horizontal bars inside of the boxes indicate medians. There were significant differences between both CBV and CBF of the tumor and white matter ($p < 0.0001$).

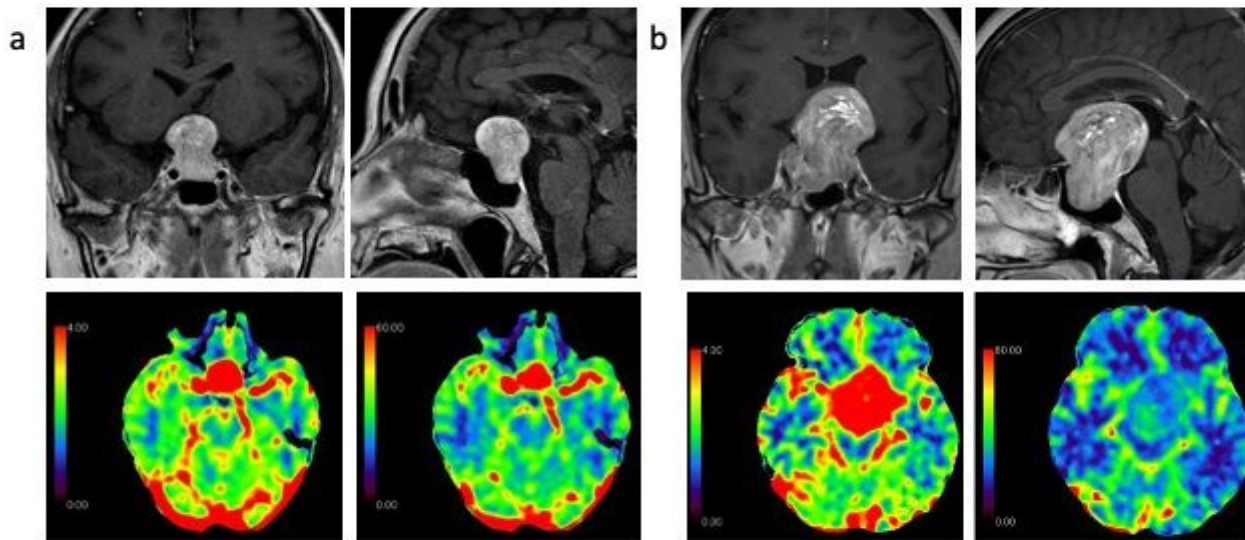


Figure 2

Representative images of patients in the high CBF (a) and low CBF (b) groups. Preoperative gadolinium-enhanced coronal and sagittal T1-weighted images (upper panel, left and right, respectively) and scaled color maps for CBV (lower panel, left) and CBF (lower panel right).

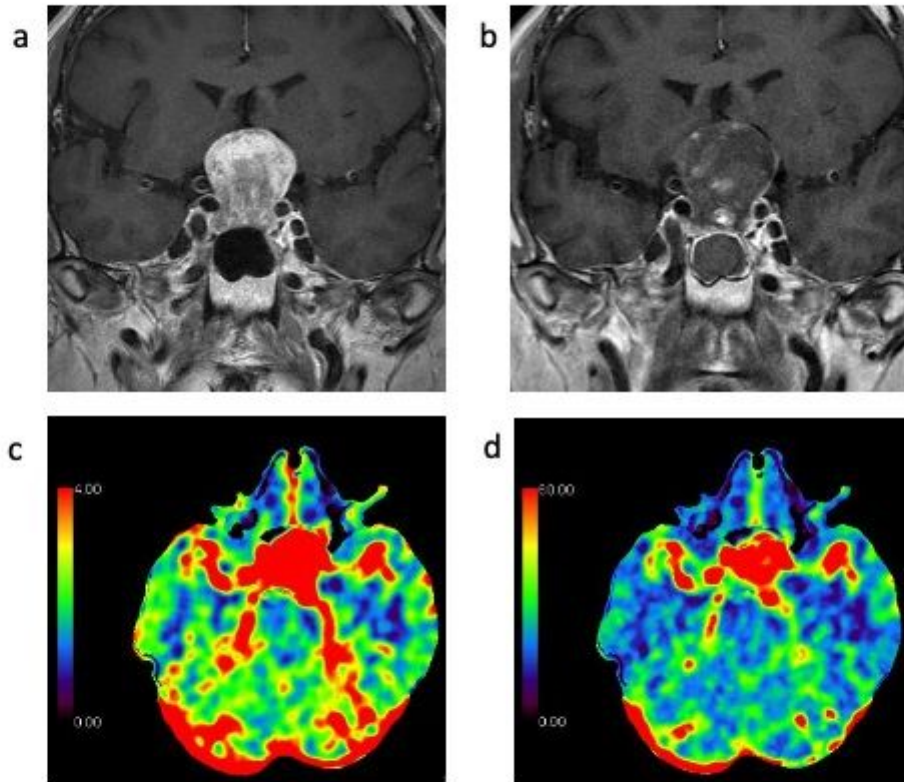


Figure 3

Preoperative (a) and postoperative (b) coronal gadolinium-enhanced T1-weighted images showing expansion of the tumor due to postoperative hemorrhage. Scaled color maps for CBV (c) and CBF (d) showing greater CBV and CBF of the tumor.